

Reactivity of Metaphosphate and Thiometaphosphate in Water: A DFT Study

Lidong Zhang and Daiqian Xie*

Department of Chemistry and Institute of Theoretical and Computational Chemistry, Nanjing University, Nanjing 210093, China

Dingguo Xu and Hua Guo*

Department of Chemistry, University of New Mexico, Albuquerque, New Mexico 87131

Received: August 8, 2005; In Final Form: September 26, 2005

Metaphosphate is known to be highly reactive to water, whereas thiometaphosphate is relatively stable in aqueous solution. The difference in their reactivity has important mechanistic implications in interpreting the “thio effect” in phosphoryl transfer reactions. In this work, density functional theory is used to investigate the reactivity of both metaphosphate and its thio-substitute in their complexes with one, two, and three waters, and in aqueous solution. Barrier heights for converting metaphosphate to orthophosphate have been determined by geometry optimization. The results confirm that metaphosphate is consistently more reactive than thiometaphosphate and the activation free energy for both species decreases with the number of water molecules. The relative stability of thiometaphosphate is attributed to its less positively charged phosphorus atom.

I. Introduction

Phosphoryl ($-\text{PO}_3^{2-}$) transfer reactions figure prominently in biochemistry because of their essential role in energy conversion, cell signaling, and the synthesis and decomposition of DNA/RNA.^{1–3} Extensive mechanistic studies have been reported for such reactions in solutions^{4–9} and in enzymes.^{8,10–12} Three limiting mechanisms can be defined by the relative timing of the nucleophilic addition (NA) and elimination (E) steps. The concerted mechanism features a bipyramidal transition state formed by synchronous NA and E steps, whereas the stepwise associative mechanism is characterized by a pentacoordinated phosphorane intermediate flanked by the transition states for the NA and E steps. In the dissociative mechanism, the metaphosphate (PO_3^-) intermediate is thought¹³ to form and subsequently react with the nucleophile. The reaction pathway adopted by a particular transphosphorylation reaction is influenced by many factors such as nucleophilicity, leaving-group mobility, protonation state, presence of metal ions, solvation, and so forth.

Reaction pathways followed by phosphate monoesters tend to proceed via a loose “metaphosphate-like” transition state, if not through a metaphosphate intermediate. For dianions, the transition state typically has significant bond cleavage to the leaving group and little bond formation with the nucleophile.^{6,11,14} For monoanions, on the other hand, proton transfer from the phosphoryl group to the leaving group often accompanies the loose transition state.^{15,16} The dominance of the concerted mechanism with a loose transition state in hydrolysis of phosphate monoesters has been confirmed by various theoretical models.^{17–20}

However, the fully dissociative scenario involving a discrete metaphosphate intermediate is rare.^{21,22} One such case is the solvolysis of the chiral *p*-nitrophenyl phosphate in aprotic solvents, in which stereochemical evidence suggested the

existence of a discrete metaphosphate intermediate.^{23,24} Several enzymatic reactions also implicated metaphosphate as an intermediate.^{25,26} On the other hand, there is ample evidence that the hydrolysis of monoesters of phosphate with a sulfur substitution in a nonbridging position (also known as phosphorothioate) is more likely to proceed via the fully dissociative mechanism involving a free thiometaphosphate. This is supported by a large extent of racemization observed in the solvolysis of chiral *p*-nitrophenyl phosphorothioate^{27–30} and by kinetic isotope effects in the hydrolysis of a thio-substituted phosphate monoester (*p*-nitrophenyl phosphorothioate).³¹

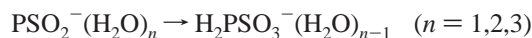
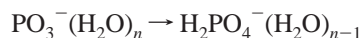
The isolation of metaphosphate in water has not been achieved, presumably because of its high tendency to react with solvent. However, gas-phase experiments have observed free metaphosphate and its complexes with a few water molecules.^{32,33} Furthermore, it was noted that the hydration energy changes when the third water is added,³⁴ which might imply a chemical change of the metaphosphate–water complex. On the other hand, thio-substituted metaphosphate is known to be much more long-lived in condensed phases. This notion is supported by the aforementioned complete racemization in the solvolysis of a chiral *p*-nitrophenyl phosphorothioate^{27–30} and by the report of a stable trithiometaphosphate salt.³⁵ It is believed that the stability of thiometaphosphate is at least partially responsible for the more “metaphosphate-like” transition state in the hydrolysis of phosphorothioates.¹¹

The understanding of the stability and reactivity of metaphosphate and its thio-substitute in water is important in interpreting the so-called “thio effect”, which measures the rate change upon substitution of one or more oxygen atoms in the phosphoryl group by sulfur. The thio effect has been widely used to investigate mechanisms in solution-phase and enzymatic transphosphorylation reactions.^{27,28,31,36–40} The influence of thio substitution on the reaction barrier has also been addressed by recent theoretical investigations.^{41–47} Nonetheless, a complete understanding of the thio effect has not been achieved. The

* Corresponding authors. E-mail: dqxie@nju.edu.cn (Xie); hguo@unm.edu (Guo).

relative stability of the metaphosphate and thiometaphosphate in water might shed valuable light on this important issue.

Although ab-initio studies of the reactivity of metaphosphate have been reported before,^{48–51} to our best knowledge, there has not been any theoretical investigation of the reactivity of thiometaphosphate. In this publication, we present density functional theory (DFT) studies on the reactivity of both metaphosphate and its thio-substituted counterpart in water clusters and in aqueous solution. We start by considering the following reactions for metaphosphate and thiometaphosphate complexed with one, two, and three waters:



We then investigate the above reactions in bulk water. The inclusion of explicit water molecules in studying reaction pathways has been shown to be necessary in many systems,^{19,52–55} particularly when proton transfer is involved. (We note in passing that OH^- may also serve as the nucleophile in alkaline solutions and in some biological systems.) These results will help us to understand the stability of thiometaphosphate in water and its mechanistic implications in phosphoryl transfer reactions. This paper is organized as follows. The theoretical models and computational details are outlined in Section II. The results are presented in Section III and discussed in Section IV. A short summary is provided in Section V.

II. Computational Details

All Becke3-Lee-Yang-Parr (B3LYP)^{56,57} calculations were performed with the Gaussian 03 package.⁵⁸ Various models for the metaphosphate–water complexes were constructed. The geometries of the reactant, product, and transition states were first optimized at the B3LYP/6-31+G(d) level and then at the B3LYP/6-311++G(d,p) level. The resulting stationary points were confirmed by frequency calculations, which also allowed the inclusion of the zero-point energy (ZPE) corrections and the calculation of thermodynamic properties. The intrinsic reaction coordinate (IRC)^{59,60} calculations were then carried out to establish the connectivity to the reactant and product. Atomic charges were obtained using the CHelpG method.⁶¹ The 6-311++G(d,p) basis set is similar to that used by York and co-workers in studying biologically relevant phosphorus-containing molecules.⁶² Because the conclusions are qualitatively the same for the two basis sets, only the latter results are reported here. To examine the solvent effect at room temperature (298 K), the polarized continuum model (PCM)⁶³ was used with $\epsilon = 80$ and the UAKS radii. The structures in the PCM calculations were not further optimized. The PCM model has been extensively used in studying phosphorus-containing molecules, and the latest results indicated that it reasonably reproduces the experimental solvation energy for several such compounds.⁶²

III. Results

A. Isolated PO_3^- and PSO_2^- Anions. The optimized structures of metaphosphate and thiometaphosphate are illustrated in Figure 1 with the CHelpG charges. The calculated geometry of metaphosphate is in good agreement with previous theoretical results.^{46,48,62} For example, the P–O bond length of 1.503 Å can be compared with 1.498 Å at the CCSD/DZP+diff level of theory.⁴⁸ For thiometaphosphate, the geometry ($r(\text{P–O}) = 1.499$ Å, $r(\text{P–S}) = 1.985$ Å) is also similar to

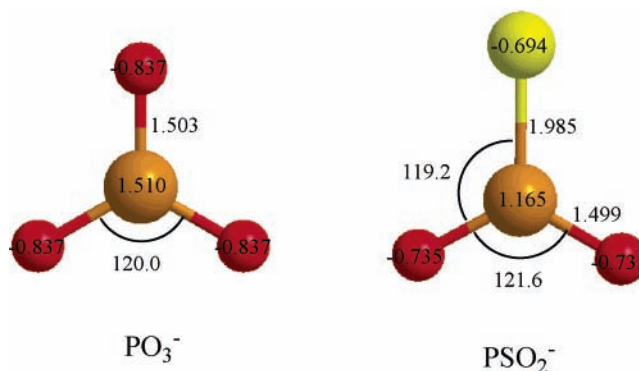


Figure 1. Equilibrium geometries of metaphosphate (PO_3^-) and thiometaphosphate (PSO_2^-) obtained at the B3LYP/6-311++G(d,p) level of theory. The bond lengths, bond angles, and CHelpG charges are also indicated in the figure.

previous theory results ($r(\text{P–O}) = 1.469$ Å, $r(\text{P–S}) = 1.971$ Å) at a lower level of theory.⁴² The change of the P–O bond length upon thio-substitution is quite small ($\Delta r = 0.004$ Å), which indicates little change in the bonding characteristics. This is consistent with observations from previous theoretical studies.^{41,42}

However, the charges of the oxygen atoms change from $-0.837e$ in PO_3^- to $-0.735e$ in PSO_2^- , whereas the phosphorus charge changes from $1.510e$ to $1.165e$. These changes are consistent with the trend observed in previous theoretical work of Basch et al.⁴² The reduced negative charges of the oxygen atoms are expected to reduce the strength of hydrogen-bond interactions with water molecules, whereas the smaller positive charge in P might reduce its electrophilicity.

B. $\text{PO}_3^-/\text{PSO}_2^- (\text{H}_2\text{O})_n$ Complexes. The complex of PO_3^- with a single water molecule (**1**) features a five-centered cyclic structure with two double donor–double acceptor hydrogen bonds, as shown in Figure 2. This structure is similar to that found in previous theoretical work on the $\text{PO}_3^- (\text{H}_2\text{O})$ complex.^{48,50,51} For $\text{PSO}_2^- (\text{H}_2\text{O})$, two structures exist, in which the water molecule forms hydrogen bonds with either two oxygen atoms (**1'**) or one oxygen and the sulfur (**1''**). Both structures are shown in Figure 2. The latter was found to be slightly lower in free energy at the B3LYP/6-311++G(d,p) level of theory. Because of the bulkier size of S, the $\text{H}\cdots\text{S}$ hydrogen bond in **1''** is longer (2.911 Å) than that between H and O (1.937 Å). Both **1** and **1'** have C_{2v} symmetry, but the $\text{H}\cdots\text{O}$ distance of 2.107 Å in the $\text{PO}_3^- (\text{H}_2\text{O})$ complex is elongated to 2.142 Å in the $\text{PSO}_2^- (\text{H}_2\text{O})$ complex, indicating weaker hydrogen bonds. This is due apparently to the smaller oxygen charges in thiometaphosphate as discussed in Section IIIA.

Two stable geometries were found for the $\text{PO}_3^- (\text{H}_2\text{O})_2$ complex and displayed in Figure 2. The first one (**2**), which has been identified before,^{48,50,51} features a bicyclic C_{2v} arrangement where metaphosphate forms four double donor–double acceptor hydrogen bonds with the two water molecules. The other structure (**3**), which is slightly higher in energy, has not been reported before. In this cyclic structure, the three constituent molecules form three hydrogen bonds, one of which is particularly strong judging from the $\text{H}\cdots\text{O}$ distance of 1.736 Å.

Four stable structures were found for the $\text{PSO}_2^- (\text{H}_2\text{O})_2$ complex, which correspond to the two structures of the $\text{PO}_3^- (\text{H}_2\text{O})_2$ complex discussed above. As shown in Figure 2, **2'** and **2''** are bicyclic arrangements similar to **2**, but differ in the dual hydrogen-bond acceptor. As in the case of single water

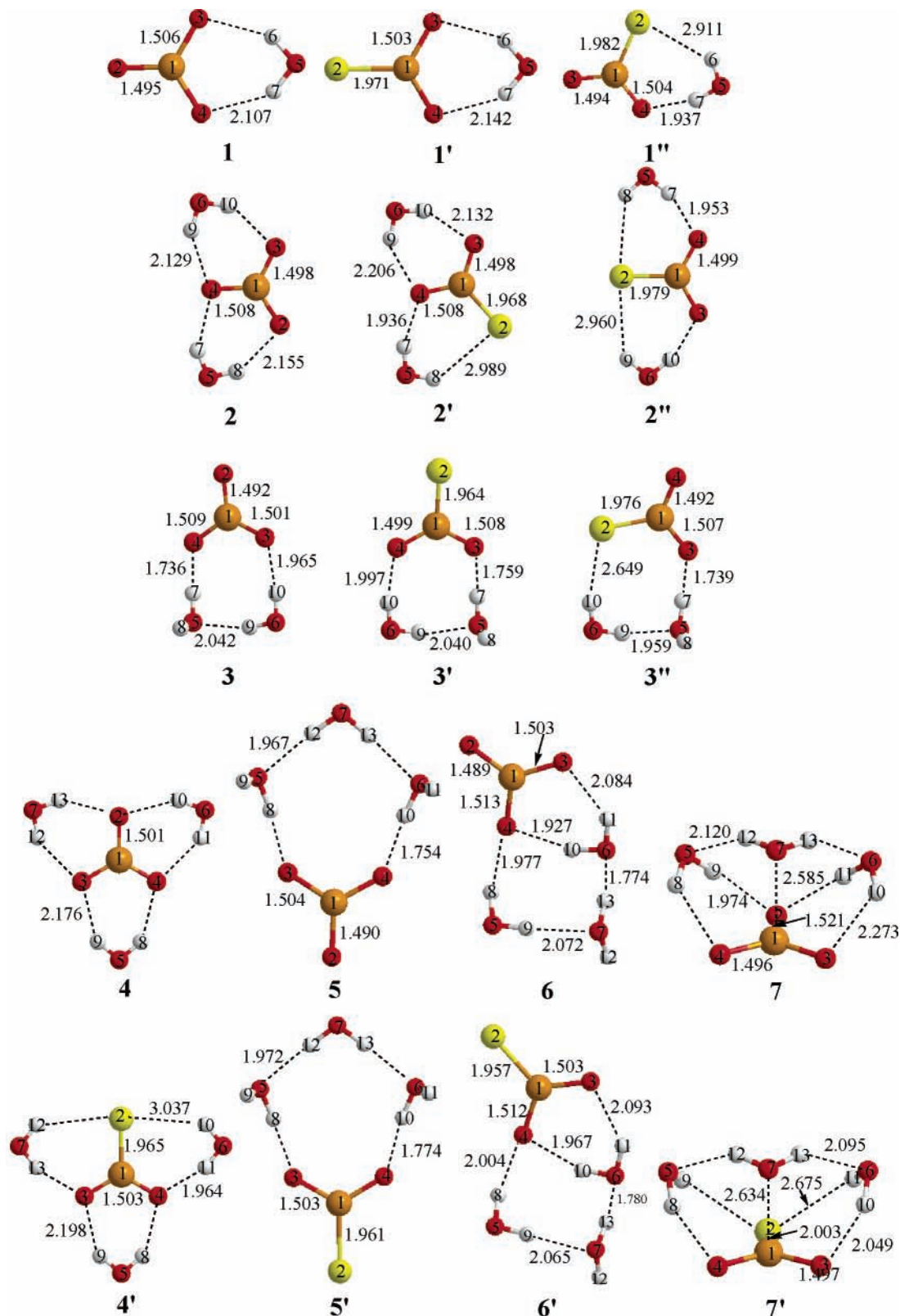


Figure 2. Geometries of the reactant complexes, $\text{PO}_3^-(\text{H}_2\text{O})_n$ and $\text{PSO}_2^-(\text{H}_2\text{O})_n$. The hydrogen, oxygen, sulfur, and phosphorus are in gray, red, yellow, and brown, respectively.

complexes, the latter with the hydrogen-bonded sulfur is the global minimum in the free energy hyper-surface. As expected, the $\text{H}\cdots\text{O}$ hydrogen-bond lengths are slightly longer (2.132 and 2.206 Å) than those in **2** (2.129 and 2.155 Å), again due to the smaller oxygen charges in PSO_2^- . On the other hand, **3'** and **3''**, shown in the same figure, are the counterparts for the cyclic structure **3** and have significantly higher free energies. These

complexes also have a very strong hydrogen bond between a water molecule and a phosphoryl oxygen.

Four stable structures were found when PO_3^- complexes with three water molecules, all displayed in Figure 2. The D_{3h} tricyclic structure **4** has six double donor–double acceptor hydrogen bonds, which can be formed by adding one water to **2**. This highly symmetric structure has been identified as the

TABLE 1: Relative Energies ΔE_{gas} (with ZPE) and Free Energies ΔG_{gas}^0 at B3LYP/6-311++G(d,p) Level for the Water Complexes in the Gas Phase^a (Labels in parentheses correspond to structures in Figures 2, 3, and 4.)

species	reactant complex $\Delta E_{\text{gas}}/\Delta G_{\text{gas}}^0$	transition state $\Delta E_{\text{gas}}/\Delta G_{\text{gas}}^0$	product complex $\Delta E_{\text{gas}}/\Delta G_{\text{gas}}^0$
$\text{PO}_3^-(\text{H}_2\text{O})$	0.00/0.00 (1)	22.66/23.97 (15)	-7.78/-6.48 (8)
$\text{PSO}_2^-(\text{H}_2\text{O})$	0.00/0.00 (1')	25.47/27.64 (15')	-4.72/-2.89 (8')
$\text{PSO}_2^-(\text{H}_2\text{O})$	0.10/0.78 (1'')	25.67/27.85 (15'')	-4.08/-2.06 (8'')
$\text{PO}_3^-(\text{H}_2\text{O})_2$	0.00/0.00 (2)	21.73/23.35 (16)	-10.37/-8.55 (9)
$\text{PO}_3^-(\text{H}_2\text{O})_2$	0.10/0.04 (3)	14.39/16.97 (17)	-10.23/-8.36 (10)
$\text{PSO}_2^-(\text{H}_2\text{O})_2$	0.00/0.00 (2')	24.56/26.69 (16')	-6.78/-5.24 (9')
$\text{PSO}_2^-(\text{H}_2\text{O})_2$	0.10/0.08 (2'')	24.55/26.57 (16'')	-6.59/-5.17 (9'')
$\text{PSO}_2^-(\text{H}_2\text{O})_2$	-0.09/0.49 (3')	17.17/20.20 (17')	-4.12/-1.13 (10')
$\text{PSO}_2^-(\text{H}_2\text{O})_2$	1.10/1.23 (3'')	16.94/20.84 (17'')	-4.05/-0.92 (10'')
$\text{PO}_3^-(\text{H}_2\text{O})_3$	-0.57/0.14 (4)	20.25/22.46 (18)	-13.12/-11.62 (11)
$\text{PO}_3^-(\text{H}_2\text{O})_3$	0.00/0.00 (5)	9.91/14.17 (19)	-13.70/-10.68 (12)
$\text{PO}_3^-(\text{H}_2\text{O})_3$	1.65/2.92 (6)	22.16/25.96 (20)	-12.48/-8.67 (13)
$\text{PO}_3^-(\text{H}_2\text{O})_3$	5.05/7.45 (7)	9.76/14.20 (21)	-13.85/-10.90 (14)
$\text{PSO}_2^-(\text{H}_2\text{O})_3$	0.00/0.00 (4')	23.79/27.04 (18')	-7.46/-4.09 (11')
$\text{PSO}_2^-(\text{H}_2\text{O})_3$	-0.05/1.54 (5')	13.36/19.29 (19')	-4.78/-1.09 (12')
$\text{PSO}_2^-(\text{H}_2\text{O})_3$	1.73/4.46 (6')	25.61/30.84 (20')	-7.92/-2.50 (13')
$\text{PSO}_2^-(\text{H}_2\text{O})_3$	6.98/11.08 (7')	15.26/21.02 (21')	-6.41/-2.19 (14')

^a Energies are given in the unit of kcal/mol, and they are referenced to the species with the lowest free energy in each complex.

global energy minimum by previous theoretical studies,^{48,50} which is confirmed by our results shown in Table 1. However, **5** has a slightly lower free energy, featuring a cyclic structure with four hydrogen bonds, two of which are very strong. **6** is a bicyclic structure with five hydrogen bonds, whereas **7** is a nonplanar structure with six hydrogen bonds. As shown in Table 1, these two structures are significantly higher in both energy and free energy than the first two.

We have found four minima for the $\text{PSO}_2^-(\text{H}_2\text{O})_3$ complex, **4'**, **5'**, **6'**, and **7'** in Figure 2, corresponding to the four $\text{PO}_3^-(\text{H}_2\text{O})_3$ structures discussed above. However, their energy order is quite different, with structure **5'** as the global minimum, as shown in Table 1.

C. $\text{H}_2\text{PO}_4^-/\text{H}_2\text{PSO}_3^-(\text{H}_2\text{O})_{n-1}$ Complexes. PO_3^- or PSO_2^- can react with a water molecule in the complexes to form dihydrogen orthophosphate or the corresponding thio-substitute. Such reactions are moderately exothermic, thus providing the thermodynamic driving force for their instability in aqueous solution. We have determined the structures and energies of the product complexes of such reactions, and the results are given in Figure 3 and Table 1.

The optimized structure of orthophosphate (**8**) has a tetrahedral phosphoryl center with C_2 symmetry, as shown in Figure 3. The P–O bond length depends on the protonation of the oxygen. The HO groups form intramolecular hydrogen bonds with the other two oxygen atoms, although they are quite weak because of the long P–OH bonds. The geometry obtained in this work is essentially the same as those reported earlier.^{49,50} For its thio-substituted counterpart, the tetrahedral phosphoryl center is similar, but there are two slightly different conformations (**8'** and **8''**), depending on the orientation of the two OH bonds. Their energies are nearly the same, as shown in Table 1.

When one water is present, the lowest energy conformation for $\text{H}_2\text{PO}_4^-(\text{H}_2\text{O})$ (**9**) features a cyclic structure, as shown in Figure 3. Double donor–double acceptor hydrogen bonds are formed between the water and the unprotonated phosphoryl oxygens, which are more negatively charged. An alternative but higher energy arrangement (**10**) is possible with the water donating a hydrogen bond to an orthophosphate O while accepting one from one of its OH group. Corresponding to **9**, there are two $\text{H}_2\text{PSO}_3^-(\text{H}_2\text{O})$ structures (**9'** and **9''**), differing

in the orientation of one OH bond. Similarly, there are two other $\text{H}_2\text{PSO}_3^-(\text{H}_2\text{O})$ structures (**10'** and **10''**) that are related to **10**. The latter two have relatively high energies when compared with the double donor–double acceptor structures (**9'** and **9''**).

The product complex for the reaction of $\text{PO}_3^-(\text{H}_2\text{O})_3$ has four different structures (**11**, **12**, **13**, and **14**), as shown in Figure 3. Similarly, four structures were found for the products of $\text{PSO}_2^-(\text{H}_2\text{O})_3$. The most stable species **11** and **11'** are clearly the product of **4** and **4'**, respectively, but the hydrogen bonds in these complexes become asymmetric because of the protonation of phosphoryl oxygens. The other pairs are also similar in the overall arrangement of the complex and in the hydrogen-bond pattern.

As shown in Table 1, the exothermicity of the reaction generally increases with the number of water molecules in the reactant complex, and the exothermicity is typically larger for metaphosphate complexes.

D. Transition States. In all the cases we have investigated, only one transition state was found between a reactant complex and a product complex, which are connected by a single IRC. As shown in Figure 4, the transition state for converting the $\text{PO}_3^-(\text{H}_2\text{O})$ complex (**1**) to orthophosphate (**8**) has a four-centered structure (**15**) with partially formed O–H and O–P bonds. Both the structure and free energy barrier height (23.97 kcal/mol) are in good accord with previous theoretical work.^{49,50} These results are also consistent with the experimental findings that indicated that metaphosphate is not reactive to water in the gas phase.³³ Two similar transition state structures (**15'** and **15''**) were found for the $\text{PSO}_2^-(\text{H}_2\text{O})$ complex, one with an OH group pointing to an O in PSO_2^- and the other pointing to S. Their energies are similar, and both are higher than that for the $\text{PO}_3^-(\text{H}_2\text{O})$ complex. These two saddle points are associated with **1'** and **1''** on the reactant side and **8'** and **8''** on the product side.

The four-centered transition states depict two events in concert: the protonation of a phosphoryl oxygen and the nucleophilic attack of the phosphorus by the oxygen in the dissociating water. As a result, the transition state contains substantial zwitterionic characteristics. The dissociating water is in a plane almost parallel to the metaphosphate, allowing its lone-pair electrons to approach the positively charged phosphorus. We believe that the higher barrier in thiometaphosphate is a manifestation of the smaller positive charge of the central phosphorus atom resulting from the sulfur substitution.

A four-centered transition state (**16**) also exists for the $\text{PO}_3^-(\text{H}_2\text{O})_2$ complex, responsible for conversion of **2** to **9**. The extra water forms double donor–double acceptor hydrogen bonds with the remaining phosphoryl oxygens, as shown in Figure 4. The resulting solvation of the transition state does not seem to affect its energy significantly, as the barrier height is about the same as that in the $\text{PO}_3^-(\text{H}_2\text{O})$ case.

A transition state of a substantially lower energy has also been identified. However, it involves six atoms in the three molecules, as shown in Figure 4 as **17**. It differs from the four-centered transition state in that the proton transfer from the water nucleophile to the phosphoryl oxygen is indirect through another water molecule that is hydrogen-bonded with both the nucleophilic water and PO_3^- . This six-centered transition state is associated with reactant complex **3** and product complex **10**, and has also some zwitterionic character. Both transition states have been reported before in earlier theoretical studies.^{49–51} The lower energy barriers corresponding to such transition states can be attributed to a more favorable geometric and electrostatic arrangement.

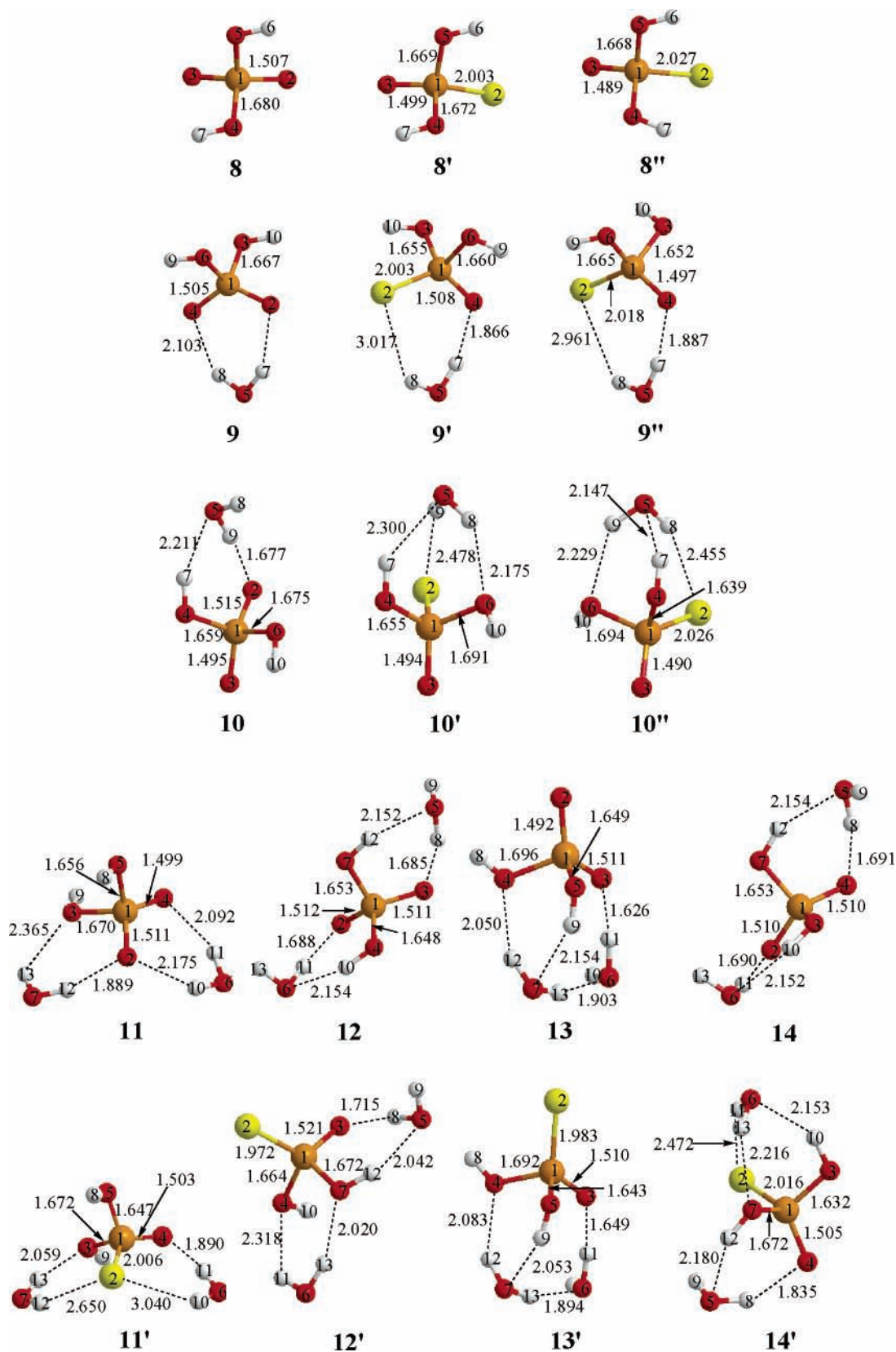


Figure 3. Geometries of the product complexes, $\text{H}_2\text{PO}_4^-(\text{H}_2\text{O})_{n-1}$ and $\text{H}_2\text{PSO}_3^-(\text{H}_2\text{O})_{n-1}$. The hydrogen, oxygen, sulfur, and phosphorus are in gray, red, yellow, and brown, respectively.

We have identified two four-centered transition states ($16'$ and $16''$) for the $\text{PSO}_2^-(\text{H}_2\text{O})_2$ reaction, as shown in Figure 4. Their energies are quite similar, and the only structural difference is in the orientation of the OH moiety in the attacking

water. IRC calculations assigned them to $2'$ and $2''$ on the reactant side and $9'$ and $9''$ on the product side, in which the same conformational difference exists. Two six-centered transition states ($17'$ and $17''$) have also been found, which relate to

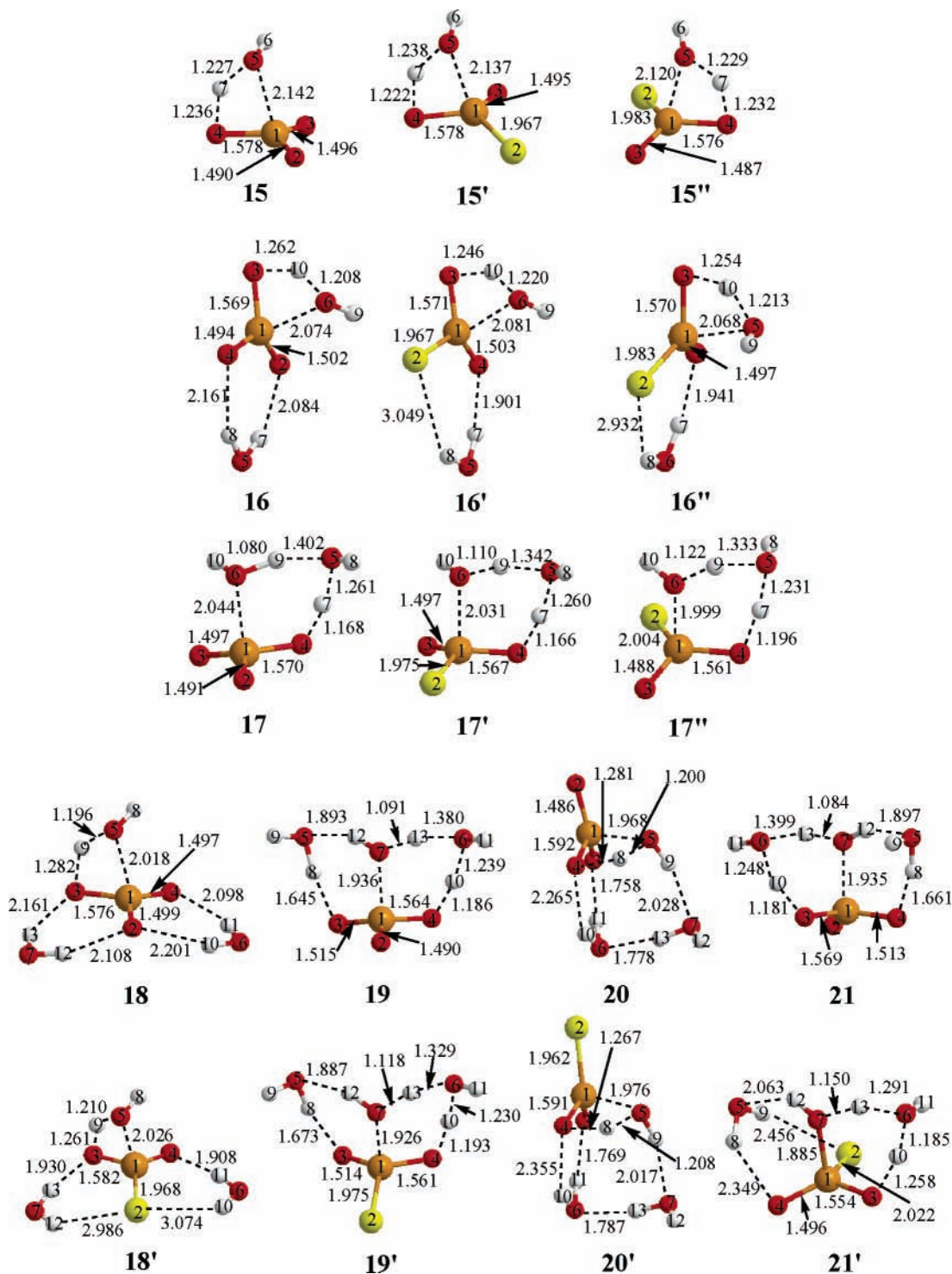


Figure 4. Geometries of the transition states. The hydrogen, oxygen, sulfur, and phosphorus are in gray, red, yellow, and brown, respectively.

3' and 3'' and 10' and 10'', respectively. As in the $\text{PO}_3^-(\text{H}_2\text{O})_2$ case, they have lower energies than the corresponding four-centered transition states.

As in smaller water complexes, the highest reaction barrier is associated with a four-centered transition state for the $\text{PO}_3^-(\text{H}_2\text{O})_3$ and $\text{PSO}_2^-(\text{H}_2\text{O})_3$ complexes. The similarities between **18** and **16** and between **18'** and **16'** are illustrated in Figure 4. The solvation of the transition state by the second water has also a relatively minor impact on the energy, as shown in Table 1. Similar to smaller complexes, the six-centered transition states (**19** and **19'**) are much lower in energy than the four-centered ones. The resemblance between **17** and **19** is

apparent, the latter having one more water. Their energies in Table 1 indicate that the lowering of the barrier by an additional water molecule is more than that for a four-centered transition state. This is easily understood because the additional water molecule interacts strongly with a reactive water molecule, whereas in the four-centered case the interaction is indirect.

20 is a four-centered transition state that correlates to the bicyclic $\text{PO}_3^-(\text{H}_2\text{O})_3$ reactant complex **6** and product complex **13**. Its barrier height is close to **18**, but with a quite different hydrogen-bond pattern. The last transition state for the $\text{PO}_3^-(\text{H}_2\text{O})_3$ complex (**21**) is a six-centered one, which connects **7** and **14**. Similar transition states (**20'** and **21'**) were found

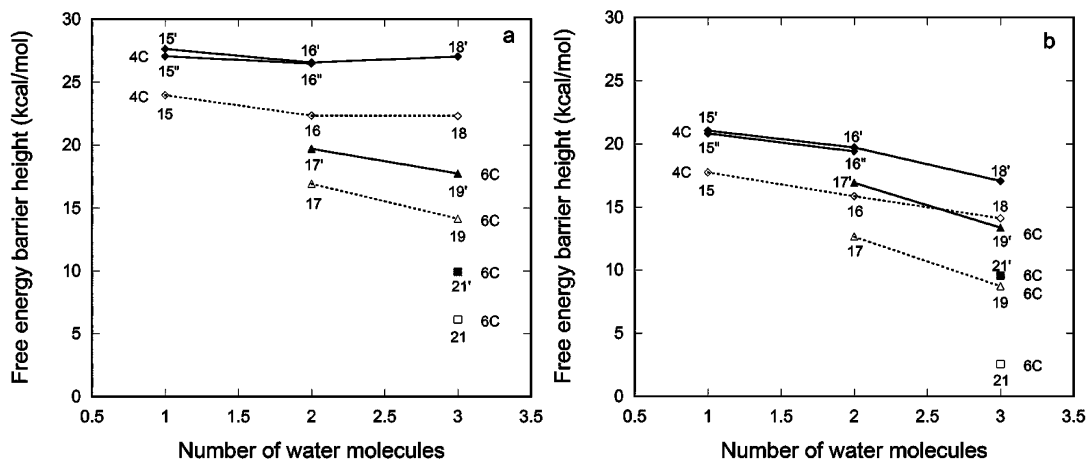


Figure 5. Free energy barriers as a function of the number of explicit water molecules in the gas phase (a) and in aqueous solution (b). The type of transition state is labeled as 4C (four-centered) or 6C (six-centered), and the data for metaphosphate and thiometaphosphate are drawn in solid and dotted lines, respectively.

between 6' and 13' and between 7' and 14' of the $\text{PSO}_2^-(\text{H}_2\text{O})_3$ complex.

Figure 5a is a plot of the free energy barrier height as a function of the number of waters in the complex. Two observations can be readily made. First, the barrier height for each type of transition state decreases with the number of waters in the complex, underscoring the effect of preferential solvation on the transition state. Second, for a given type of transition state, the energy barrier for converting metaphosphate to orthophosphate is consistently lower than that for converting thiometaphosphate because of the reduced positive charge at the phosphorus of thiometaphosphate, which renders the nucleophilic attack by the OH^- less favorable. In the section that follows, further evidence will be presented to support this conclusion.

E. Bulk Solvent Effect. The dependence of the reaction barrier height on the number of water molecules in the complex suggests that solvation plays an indispensable role in the reactivity of metaphosphate and its thio-substitute. Because further additions of explicit water molecules become more difficult computationally, we report in Table 2 the energetics of gas-phase stationary points augmented by solvation free energy obtained from an implicit solvent model, namely PCM. These energies were obtained without further optimization of the complex structures. The data in Table 2 indicate that solvation of the complexes drastically changed the energy order. For example, 5 is almost isoenergetic with 4 in the gas phase, but in solution it is about 10 kcal/mol lower in energy. This can be readily understood because 5 has a more exposed metaphosphate and thus is more susceptible to solvent stabilization.

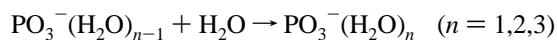
Figure 5b displays the barrier height of the solvated systems as a function of the number of explicit water molecules included in the model. As in Figure 5a, the barrier height typically decreases with the number of water molecules in the model. More importantly, the barriers are much lower than their gas-phase counterparts shown in Figure 5a, underscoring the lowering of transition-state energies by bulk solvation. This is not surprising, as the transition states have strong zwitterionic characters resulting from the dissociation of the water nucleophile to a proton and a hydroxide. These figures also show that the lowest barriers in solution are associated with a six-centered transition states, namely 21 and 21'. They are expected to dominate the solution reaction pathways with their negligible 2.57 and 9.57 kcal/mol barriers.

TABLE 2: Relative Free Energies (ΔG_{sol}^0) in Aqueous Solution and Barrier Height Calculated Using the PCM Model with UAKS Radii at the B3LYP/6-311++G(d,p) Level^a (Labels in parentheses correspond to structures in Figures 2, 3, and 4.)

species	reactant complex ΔG_{sol}^0	transition state ΔG_{sol}^0	product complex ΔG_{sol}^0	barrier height (kcal/mol)
$\text{PO}_3^-(\text{H}_2\text{O})$	0.00 (1)	17.75 (15)	-17.62 (8)	17.75
$\text{PSO}_2^-(\text{H}_2\text{O})$	0.00 (1')	21.06 (15')	-10.86 (8')	21.06
$\text{PSO}_2^-(\text{H}_2\text{O})$	0.28 (1'')	21.10 (15'')	-11.15 (8'')	20.82
$\text{PO}_3^-(\text{H}_2\text{O})_2$	0.00 (2)	15.87 (16)	-20.11 (9)	15.87
$\text{PO}_3^-(\text{H}_2\text{O})_2$	-5.34 (3)	7.30 (17)	-21.71 (10)	12.64
$\text{PSO}_2^-(\text{H}_2\text{O})_2$	0.00 (2')	19.72 (16')	-13.80 (9')	19.72
$\text{PSO}_2^-(\text{H}_2\text{O})_2$	0.11 (2'')	19.52 (16'')	-13.25 (9'')	19.41
$\text{PSO}_2^-(\text{H}_2\text{O})_2$	-4.88 (3')	12.04 (17')	-12.09 (10')	16.92
$\text{PSO}_2^-(\text{H}_2\text{O})_2$	-3.79 (3'')	11.77 (17'')	-12.38 (10'')	15.56
$\text{PO}_3^-(\text{H}_2\text{O})_3$	9.69 (4)	23.81 (18)	-13.26 (11)	14.12
$\text{PO}_3^-(\text{H}_2\text{O})_3$	0.00 (5)	8.72 (19)	-16.61 (12)	8.72
$\text{PO}_3^-(\text{H}_2\text{O})_3$	3.98 (6)	20.05 (20)	-16.43 (13)	16.07
$\text{PO}_3^-(\text{H}_2\text{O})_3$	6.85 (7)	9.42 (21)	-16.48 (14)	2.57
$\text{PSO}_2^-(\text{H}_2\text{O})_3$	0.00 (4')	17.72 (18')	-15.09 (11')	17.72
$\text{PSO}_2^-(\text{H}_2\text{O})_3$	-9.30 (5')	4.08 (19')	-15.72 (12')	13.38
$\text{PSO}_2^-(\text{H}_2\text{O})_3$	-5.40 (6')	14.54 (20')	-19.48 (13')	19.94
$\text{PSO}_2^-(\text{H}_2\text{O})_3$	-0.48 (7')	9.09 (21')	-14.12 (14')	9.57

^a Energies are given in the unit of kcal/mol, and they are referenced to the species with the lowest free energy in each complex in Table 1.

F. Energetics of Complex Formation. The changes in energy, enthalpy, free energy, and entropy for the formation of metaphosphate-water complexes:



are compiled in Table 3 with comparison with available experimental data. These processes are most likely barrierless. Because multiple minimum-energy structures were involved, choices have to be made in calculating these thermodynamic properties. We have elected to compute these quantities from the global free energy minima, because the Boltzmann factor discriminates high energy structures. The calculated free energy changes indicate that exothermicity decreases with the number (n) of water molecules in the complex. The overall agreement with the experimental data³⁴ is satisfactory, although we notice that the exothermicity for $n = 3$ is much smaller than the experimental value. This observation is consistent with theoretical results reported earlier by other groups.^{48,50} On the basis of

TABLE 3: Calculated Changes in the Energy (ΔE , kcal/mol), Enthalpy (ΔH^0 , kcal/mol), Free Energy (ΔG^0 , kcal/mol), and Entropy (ΔS^0 , cal/mol K) of the Hydration Reactions, and Comparison with Experimental Data of Keesee and Castleman^a

no. of H ₂ O	ΔE	ΔH^0	ΔS^0	ΔG^0
$\text{PO}_3^-(\text{H}_2\text{O})_{n-1} + \text{H}_2\text{O} \rightarrow \text{PO}_3^-(\text{H}_2\text{O})_n$				
$n = 1$, theo.	-12.73	-13.32	-26.46	-5.43
$n = 1$, exp.		-12.9	-22.3	-6.3
$n = 2$, theo.	-11.01	-11.60	-27.42	-3.42
$n = 2$, exp. ^b		-11.4	-22.0	-4.9
$n = 2$, theo.	-9.39	-9.98	-27.19	-1.88
$n = 2$, exp. ^b		-16.3	-36.4	-5.5
$\text{PSO}_2^-(\text{H}_2\text{O})_{n-1} + \text{H}_2\text{O} \rightarrow \text{PSO}_2^-(\text{H}_2\text{O})_n$				
$n = 1$, theo.	-11.31	-11.91	-25.49	-4.31
$n = 2$, theo.	-10.01	-10.60	-24.78	-3.21
$n = 3$, theo.	-8.79	-9.38	-22.59	-2.64

^a Ref 34. ^b Experimental data are for D₂O.³⁴

the transition-state energies listed in Table 1, our results are supportive to the conclusion of the previous theoretical work^{49,50} that the isomerization reaction in small gas-phase metaphosphate-water complexes is very unlikely. The discrepancy between the experimental and theoretical data is not yet understood.

Data for $\text{PSO}_2^-(\text{H}_2\text{O})_n$ complexes have also been calculated and listed in Table 3. As in the $\text{PO}_3^-(\text{H}_2\text{O})_n$ case, the exothermicity decreases monotonically with the number of water molecules in the complex. Unfortunately, no experimental data have been reported.

IV. Discussion

The main focus of this work is on the reactivity of metaphosphate and thiometaphosphate in water clusters and in aqueous solution. Our results presented in Section III indicated that there are two types of transition states responsible for their conversion to orthophosphates. These transition states involve either one or two water molecules, and the latter typically have lower energies. For each type of transition state, the free energy barrier height generally decreases with the number of water molecules in the complex. When three waters are involved, the lowest activation free energy drops to 6.75 and 9.94 kcal/mol for metaphosphate and thiometaphosphate, respectively. In aqueous solution, these values decrease further to 2.57 and 9.57 kcal/mol, which are consistent with the observed high reactivity of metaphosphate and relative stability of thiometaphosphate.

The six-centered transition states become available with at least two water molecules. Their role in gas-phase reactions is probably very limited because of the unfavorable entropic factor. However, access of such ter-molecular transition states for solution-phase reactions should be relatively easy. Similar transition states have been identified in other systems and shown to significantly lower the barrier height for proton-transfer reactions.⁵²⁻⁵⁴ In particular, a six-centered transition state was found to dominate the hydrolysis pathway for the monoanion of methyl phosphate.^{19,20} They underscore the importance of explicit solvent involvement in chemical reactions by lowering the proton-transfer barriers.

In all results presented in the previous section, it is clear that the reaction barrier for thiometaphosphate is significantly higher than that of metaphosphate. This is true not only for the four-centered transition states, but also for the lower energy six-centered transition states. In aqueous solution, the difference can be as large as 7 kcal/mol, which translates to approximately a 5 orders of magnitude difference in reaction rates.

One possibility for the relative stability of thiometaphosphate is the weaker hydrogen bond formed between the sulfur and solvent water. However, this explanation is not supported by our results, which showed that even with one water molecule the reaction barrier of thiometaphosphate is significantly higher than its unsubstituted counterpart. In other words, its reduced reactivity in aqueous solution is intrinsic. This observation echoes the conclusion drawn by Catrina and Hengge on the reactivity of phosphorothioates, in which the solvent effect was ruled out as a main contributor of the reduced activation energy in hydrolysis.⁴⁰

We have attributed the higher stability of thiometaphosphate in water clusters and in aqueous solution to its charge distribution, which indicates a less positively charged phosphoryl center than that in metaphosphate. The smaller positive charge of the phosphorus atom makes it more difficult for the nucleophilic attack by the hydroxide, resulting in a higher reaction barrier.

V. Conclusions

We have in this work investigated the structure of water clusters of metaphosphate and thiometaphosphate using a density functional method. Their reactivity with water to form orthophosphates was also studied by determining the reaction transition states in the gas-phase clusters and in bulk water. The latter was treated with a supermolecular approach with an implicit solvent model. Our results are consistent with previous experimental and theoretical work which showed that metaphosphate is stable in such clusters with up to three water molecules, because of relatively high reaction barriers.

However, the emergence of six-centered transition states, which become dominant when more waters become available, renders the anion very reactive in aqueous solution. Our theoretical observations are consistent with the experimental consensus^{21,22,33,34} about the stability of the metaphosphate anion in different environments. We note in passing that because a solvent water is involved in the transfer of a proton, locating such a transition state would not be possible if the solvent water is not explicitly included in the quantum chemical calculation.

In both water clusters and aqueous solution, the reactivity of thiometaphosphate is shown to be much less pronounced than that of metaphosphate. For both four-centered and six-centered transition states, the barrier height for thiometaphosphate is always higher than those for metaphosphate. The higher reaction barrier is attributed to the less positively charged phosphoryl center, whose reduced electrophilicity renders the attack by the nucleophilic water more difficult. The higher stability of thiometaphosphate in aqueous solution supports its discrete intermediacy in solution-phase reactions, as speculated in many previous experimental investigations. It might also be responsible for the more "metaphosphate-like" transition state in hydrolysis of sulfur-substituted phosphates. As a result, the theoretical results presented in this work will help us to gain deeper insight into the origin of the thio effect that has been widely used in many mechanistic studies of enzymatic phosphoryl transfer reactions.

Acknowledgment. This work was funded by the Teaching and Research Award Program for Outstanding Young Teachers in Higher Education Institutions of MOE, PRC (D.X.), and by the US NSF (MCB-30370337 to H.G.). H.G. thanks Prof. D. Dunaway-Mariano for many stimulating discussions.

References and Notes

- (1) Westheimer, F. H. *Science* **1987**, *235*, 1173.
- (2) Mildvan, A. S. *Proteins* **1997**, *29*, 401.

- (3) Oivanen, M.; Kuusela, S.; Lonnberg, H. *Chem. Rev.* **1998**, *98*, 961.
- (4) Benkovic, S. J.; Schray, K. J. Mechanisms of phosphoryl transfer. In *Transition States of Biochemical Processes*; Gandour, R. D., Ed.; Plenum: New York, 1978.
- (5) Westheimer, F. H. *Chem. Rev.* **1981**, *81*, 313.
- (6) Thatcher, G. R. J.; Kluger, R. *Adv. Phys. Org. Chem.* **1989**, *25*, 99.
- (7) Cleland, W. W.; Hengge, A. C. *FASEB J.* **1995**, *9*, 1586.
- (8) Hengge, A. C. *Acc. Chem. Res.* **2002**, *35*, 105.
- (9) Hengge, A. C.; Onyido, I. *Curr. Org. Chem.* **2005**, *9*, 61.
- (10) Knowles, J. R. *Annu. Rev. Biochem.* **1980**, *49*, 877.
- (11) Hengge, A. C. Transfer of the PO₃²⁻ group. In *Comprehensive Biological Catalysis*; Sinnott, M., Ed.; Academic Press: San Diego, 1998; Vol. 1.
- (12) Allen, K. N.; Dunaway-Mariano, D. *Trends Biochem. Sci.* **2004**, *29*, 495.
- (13) Butcher, W. W.; Westheimer, F. H. *J. Am. Chem. Soc.* **1955**, *77*, 2420.
- (14) Admiraal, S. J.; Herschlag, D. *Chem. Biol.* **1995**, *2*, 729.
- (15) Kirby, A. J.; Varvoglis, A. G. *J. Am. Chem. Soc.* **1967**, *89*, 415.
- (16) Grzyska, P. K.; Czyryca, P. G.; Purcell, J.; Hengge, A. C. *J. Am. Chem. Soc.* **2003**, *125*, 13106.
- (17) Florian, J.; Warshel, A. *J. Phys. Chem.* **1998**, *B102*, 719.
- (18) Florian, J.; Warshel, A. *J. Am. Chem. Soc.* **1998**, *120*, 11524.
- (19) Hu, C.-H.; Brinck, T. *J. Phys. Chem.* **1999**, *A103*, 5379.
- (20) Wang, Y.-N.; Topol, I. A.; Collins, J. R.; Burt, S. K. *J. Am. Chem. Soc.* **2003**, *125*, 13265.
- (21) Herschlag, D.; Jencks, W. P. *J. Am. Chem. Soc.* **1989**, *111*, 7579.
- (22) Lightcap, E. S.; Frey, P. A. *J. Am. Chem. Soc.* **1991**, *113*, 9415.
- (23) Buchwald, S. L.; Friedman, J. M.; Knowles, J. R. *J. Am. Chem. Soc.* **1984**, *106*, 4911.
- (24) Friedman, J. M.; Freeman, S.; Knowles, J. R. *J. Am. Chem. Soc.* **1988**, *110*, 1268.
- (25) Choe, J.-Y.; Iancu, C. V.; Fromm, H. J.; Honzatko, R. B. *J. Biol. Chem.* **2003**, *278*, 16015.
- (26) Liu, S.; Lu, Z.; Jia, Y.; Dunaway-Mariano, D.; Herzberg, O. *Biochemistry* **2002**, *41*, 10270.
- (27) Cullis, P. M.; Iagrossi, A. *J. Am. Chem. Soc.* **1986**, *108*, 7870.
- (28) Cullis, P. M.; Misra, R.; Wilkins, D. J. *J. Chem. Soc. Chem. Commun.* **1987**, 1594.
- (29) Domanico, P.; Mizrahi, V.; Benkovic, S. J. In *Mechanisms of Enzymatic Reactions: Stereochemistry*; Frey, P. A., Ed.; Elsevier: New York, 1986; p 127.
- (30) Burgess, J.; Blundell, T. L.; Cullis, P. M.; Hubbard, C. D.; Misra, R. *J. Am. Chem. Soc.* **1988**, *110*, 7900.
- (31) Catrina, I. E.; Hengge, A. C. *J. Am. Chem. Soc.* **2003**, *125*, 7546.
- (32) Harvan, D. J.; Hass, J. R.; Busch, K. L.; Bursey, M. M.; Ramirez, F.; Meyerson, S. *J. Am. Chem. Soc.* **1979**, *101*, 7409.
- (33) Henchman, M.; Viggiano, A. A.; Paulson, J. F.; Freedman, A.; Wormhoudt, J. *J. Am. Chem. Soc.* **1985**, *107*, 1453.
- (34) Keesee, R. G.; Castleman, A. W., Jr. *J. Am. Chem. Soc.* **1989**, *111*, 9015.
- (35) Roesky, H. W.; Ahlrichs, R.; Brode, S. *Angew. Chim. Int. Ed.* **1986**, *25*, 82.
- (36) Breslow, R.; Katz, I. *J. Am. Chem. Soc.* **1968**, *90*, 7376.
- (37) Herschlag, D.; Piccirilli, J. A.; Cech, T. R. *Biochemistry* **1991**, *30*, 4844.
- (38) Hollfelder, F.; Herschlag, D. *Biochemistry* **1995**, *34*, 12255.
- (39) Breslow, R.; Chapman, W. H. *J. Proc. Natl. Acad. Sci. U.S.A.* **1996**, *93*, 10018.
- (40) Catrina, I. E.; Hengge, A. C. *J. Am. Chem. Soc.* **1999**, *121*, 2156.
- (41) Liang, C.; Allen, L. C. *J. Am. Chem. Soc.* **1987**, *109*, 6449.
- (42) Basch, H.; Krauss, M.; Stevens, W. J. *J. Mol. Struct. (THEOCHEM)* **1991**, *235*, 277.
- (43) Zhou, D.-M.; Taira, K. *Chem. Rev.* **1998**, *98*, 991.
- (44) Gregersen, B. A.; Lopez, X.; York, D. M. *J. Am. Chem. Soc.* **2003**, *125*, 7178.
- (45) Gregersen, B. A.; Lopez, X.; York, D. M. *J. Am. Chem. Soc.* **2004**, *126*, 7504.
- (46) Xu, D.; Guo, H.; Liu, Y.; York, D. M. *J. Phys. Chem.* **2005**, *B109*, 13827.
- (47) Liu, Y.; York, D. M. *Chem. Commun.* **2005**, 3909.
- (48) Ma, B.; Xie, Y.; Shen, M.; Schaefer, H. F., III. *J. Am. Chem. Soc.* **1993**, *115*, 1943.
- (49) Ma, B.; Xie, Y.; Shen, M.; Schleyer, P. v. R.; Schaefer, H. F., III. *J. Am. Chem. Soc.* **1993**, *115*, 11169.
- (50) Wu, Y.-D.; Houk, K. N. *J. Am. Chem. Soc.* **1993**, *115*, 11997.
- (51) Mercero, J. M.; Barrett, P.; Lam, C. W.; Flower, J. E.; Ugalde, J. M.; Pedersen, L. *J. Comput. Chem.* **2000**, *21*, 43.
- (52) Fraser, R. R.; Kong, F.; Stanculescu, M.; Wu, Y. D.; Houk, K. N. *J. Org. Chem.* **1993**, *58*, 4431.
- (53) Zhan, C. G.; Landry, D. W.; Ornstein, R. L. *J. Am. Chem. Soc.* **2000**, *122*, 2621.
- (54) Xue, Y.; Kim, C. K.; Guo, Y.; Xie, D.; Yan, G. *J. Comput. Chem.* **2005**, *26*, 994.
- (55) Xie, D.; Zhou, Y.; Xu, D.; Guo, H. *Org. Lett.* **2005**, *7*, 2093.
- (56) Becke, A. D. *J. Chem. Phys.* **1993**, *98*, 5648.
- (57) Lee, C.; Yang, W.; Parr, R. G. *Phys. Rev. B* **1988**, *37*, 785.
- (58) Frisch, M. J.; Trucks, G. W.; Schlegel, H. B.; Scuseria, G. E.; Robb, M. A.; Cheeseman, J. R.; Montgomery, J. A., Jr.; T. V.; Kudin, K. N.; Burant, J. C.; Millam, J. M.; Iyengar, S. S.; Tomasi, J.; Barone, V.; Mennucci, B.; Cossi, M.; Scalmani, G.; Rega, N.; Petersson, G. A.; Nakatsuji, H.; Hada, M.; Ehara, M.; Toyota, K.; Fukuda, R.; Hasegawa, J.; Ishida, M.; Nakajima, T.; Honda, Y.; Kitao, O.; Nakai, H.; Klene, M.; Li, X.; Knox, J. E.; Hratchian, H. P.; Cross, J. B.; Adamo, C.; Jaramillo, J.; Gomperts, R.; Stratmann, R. E.; Yazyev, O.; Austin, A. J.; Cammi, R.; Pomelli, C.; Ochterski, J. W.; Ayala, P. Y.; Morokuma, K.; Voth, G. A.; Salvador, P.; Dannenberg, J. J.; Zakrzewski, V. G.; Dapprich, S.; Daniels, A. D.; Strain, M. C.; Farkas, O.; Malick, D. K.; Rabuck, A. D.; Raghavachari, K.; Foresman, J. B.; Ortiz, J. V.; Cui, Q.; Baboul, A. G.; Clifford, S.; Cioslowski, J.; Stefanov, B. B.; Liu, G.; Liashenko, A.; Piskorz, P.; Komaromi, I.; Martin, R. L.; Fox, D. J.; Keith, T.; Al-Laham, M. A.; Peng, C. Y.; Nanayakkara, A.; Challacombe, M.; Gill, P. M. W.; Johnson, B.; Chen, W.; Wong, M. W.; Gonzalez, C.; Pople, J. A. *Gaussian 03*, Revision A.1; Gaussian, Inc.: Pittsburgh, PA, 2003.
- (59) Gonzalez, C.; Schlegel, H. B. *J. Chem. Phys.* **1989**, *90*, 2154.
- (60) Gonzalez, C.; Schlegel, H. B. *J. Phys. Chem.* **1990**, *94*, 5523.
- (61) Breneman, C. M.; Wiberg, K. B. *J. Comput. Chem.* **1990**, *11*, 361.
- (62) Range, K.; McGrath, M. J.; Lopez, X.; York, D. M. *J. Am. Chem. Soc.* **2004**, *126*, 1654.
- (63) Tomasi, J.; Persico, M. *Chem. Rev.* **1994**, *94*, 2027.